Available online at www.sciencedirect.com
SCIENCE DIRECT®
Electrochemistry Communications 5 (2003) 741–746
electrochemistry communications
www.elsevier.com/locate/elecom

Enantiomeric electro-oxidation of D- and L-glucose on chiral gold single crystal surfaces

A. Martins [a,*], V. Ferreira [a], A. Queirós [a], I. Aroso [a], F. Silva [a], J. Feliu [b]

[a] Departamento de Química da Faculdade de Ciências da Universidade do Porto, R. do Campo Alegre 687, 4169-007 Porto, Portugal
[b] Department de Quimica Fisica, Universitat d'Alacant, Apartat 99, E-03080 Alacant, Spain

Received 11 June 2003; received in revised form 4 July 2003; accepted 8 July 2003
Published online: 12 August 2003

Abstract

The enantioselectivity of the gold chiral surfaces towards the electrocatalytic oxidation of D- and L-glucose in neutral phosphate-buffered media is reported. Two enantiomorphic surfaces were used, Au{3 2 1}^{R} and Au{3 2 1}^{S}, and results obtained by cyclic voltammetry were compared with two non-chiral surfaces having the same terrace and step orientations, Au(1 1 1) and Au(2 1 1). An enantioselective effect is observed, Au{3 2 1}^{R} exhibits a higher activity for D-glucose while Au{3 2 1}^{S} exhibits a higher activity for L-glucose. The corresponding enantioselectivity factor was estimated to 10% for the process occurring at lower potential values and to 50% for the process at higher potential values. These results represent the first evidence that gold chiral surfaces are capable of enantiomeric discrimination.

Keywords: Gold; Chiral surfaces; Enantioselectivity; Glucose electro-oxidation

1. Introduction

Chiral surface chemistry is an emerging field of research [1] whose driving motivation is intimately related with the synthesis and probing of chiral pharmaceuticals. Though some enantioselective surface reactions were discovered decades ago [2], chiral surface chemistry has hardly been defined, let alone explored. Chiral surface processes and reactions can proceed with high enantiospecificity, but examples are few and fundamentals are lacking. Understanding the fundamentals of 2D stereoselectivity will not only cast light upon the mechanisms involved in some already exploited heterogeneous catalytic reactions but will also help designing new chiral materials for enantioselective synthesis and sensing.

One of the possible routes to achieve 2D chiral discrimination is the use of chiral substrates such as enantiomorphic bare metal surfaces. It is indeed possible to prepare surfaces by suitable cutting of metal single crystals that are, at the atomic level, mirror images of one another and can thus be considered chiral. High Miller index surfaces composed of low Miller index flat terraces separated by kinked steps fulfil this requirement. Their handedness is defined by the surface atom density sequence of the three microfacets that form the step edges. Full description of these surfaces and details for their preparation are given elsewhere [3].

Since Gellman and coworkers first postulated, in 1996 [4], that kinked single crystal surfaces of metal ought to have enantiospecific properties, several studies have been published that evidence the intrinsic chirality of these surfaces towards adsorption and oxidation of organic chiral molecules. The first experimental evidence was observed for the enantiospecific electro-oxidation of D- and L-glucose on chiral platinum surfaces in 1999 [5,6]. The investigation on the enantioselectivity of platinum surfaces was successfully pursued [7,8], as well as on Pt/graphite [9] and Pt/Pd [10] catalysts. Despite their initial difficulties in demonstrating their prediction using *R*- and *S*-2-butanol [4], Gellman and coworkers were later able to observe the enantiospecific desorption

* Corresponding author. Tel.: +351-22-6082943; fax: +351-22-6082959.
E-mail address: amartins@fc.up.pt (A. Martins).

1388-2481/$ - see front matter © 2003 Elsevier B.V. All rights reserved.
doi:10.1016/S1388-2481(03)00182-6

of *R*- and *S*-propylene oxide and *R*-3-methyl-cyclohexanone on Cu chiral surfaces using TPD and FTIRRAS techniques [11–13]. Sholl and coworkers have also taken interest in this subject and have contributed with a theoretical approach to the study of the enantiospecific adsorption of chiral hydrocarbons on Pt and Cu chiral surfaces [14,15]. These authors have also directed their attention to the possible relaxation and reconstruction of these surfaces and their impact on their intrinsic chirality [16–19].

The electro-oxidation of glucose enantiomers was the first probe reaction that successfully showed that chiral surfaces of platinum had enantiospecific selectivity [5,6,8]. When compared with flat and stepped surfaces which are by definition deprived of enantioselective ability, these surfaces exhibit chiral discrimination that scaled with the surface density of kink sites. Although the rate of glucose adsorption and oxidation was found to increase with increasing terrace width, the diasteromeric excess for the electro-oxidation increased with increasing density of kink sites hence of chiral active centres.

Although platinum, as the electrode material, has been the subject of most of the studies on glucose electro-oxidation over the past 50 years, the pronounced poisoning platinum by some intermediates and/or products suppresses its intrinsic activity by blocking the surface electrode. Gold, however, is a generally more active electrocatalyst than platinum in neutral and alkaline electrolytes [20] and does not suffer from poisoning. Results published in the literature [21,22] reported that glucose oxidation in neutral and alkaline media is structure sensitive and that the presence of steps causes substantial changes in the activity of the surface towards glucose oxidation.

We have therefore selected the electro-oxidation of glucose enantiomers to probe the enantiospecificity of the gold chiral surfaces $Au\{3\,2\,1\}^{R}$ and $Au\{3\,2\,1\}^{S}$. The same study was also performed on two non-chiral gold surfaces, Au(1 1 1) and Au(2 1 1). Au(1 1 1) was selected for being a smooth surface with the same orientation as the terraces on Au(3 2 1). Au(2 1 1) was selected for having terraces with the same orientation and width as the terraces on Au(3 2 1) but no kinks.

So far, no experimental evidence of the enantioselectivity of gold chiral surfaces has been reported, but Žljivančanin et al. [23] recently published a DFT study on the enantioselective adsorption of (*S*) and (*R*)-2-amino-3-(dimethylphosphino)1-propanethiol on $Au\{17\,11\,9\}^{S}$ and we expect, therefore, to obtain experimental evidence of the enantiospecific properties of such surfaces.

2. Experimental

The gold bead electrodes $Au\{3\,2\,1\}^{R}$ and $Au\{3\,2\,1\}^{S}$ used in the experiments where prepared in Alicante using the Clavilier method [24]. The gold bead electrodes Au(1 1 1) and Au(2 1 1) were prepared in the CNRS-Meudon using the Hamelin method [25,26]. Pre-treatment of the gold electrodes was performed before each experiment and consisted of a flame annealing followed by quenching in ultra-pure water [27,28]. Contact with the solution was established by the hanging electrolyte method.

Cyclic voltammetry was performed with an Autolab PSTAT10 potentiostat (Ecochemie) at 50 $mV\,s^{-1}$. The counter electrode was a gold coil previously flame annealed. The reference electrode, Ag/AgCl in saturated NaCl, was kept in a separate cell containing the electrolytic solution and connected to the working electrode by a salt bridge. The capacitance measurements were performed with a Voltalab PGZ 301 potentiostat (Radiometer) using an AC sine wave with a frequency 20 Hz and 10 mV peak to peak amplitude.

Unless otherwise stated, all experiments were performed in a phosphate buffer solution, pH 7.5, containing 0.008 M NaH_2PO_4 and 0.03 M Na_2HPO_4 (p.a. Merck) and 10 mM D- or L-glucose (Fluka, purity >99.5%). The glucose solutions were prepared at least 12 h prior to the electrochemical measurements for equilibration (mutarotation) between the α- and β-glucose moieties [29]. The solutions were degassed before each experiment using purified N_2 and a constant flow was maintained over the solution during experiments. Stirring of the solutions was maintained constant during experiments for all solutions.

The reproducibility of the results, hence the glucose electro-oxidation currents, was highly affected by the shape of the hanging electrolyte meniscus. Even though a very strict control of the electrode position and contact area was attempted, variations of the current density values at the glucose oxidation peaks could amount to 3%. The final profiles presented in this study will correspond to an average curve of five stable cyclic voltammograms obtained in consecutive experiments performed under the same experimental conditions.

3. Results

3.1. Characterization of $Au\{3\,2\,1\}^{R}$ and $Au\{3\,2\,1\}^{S}$ gold surfaces

According to the "microfacet notation" introduced by Somorjai et al. [30], high Miller index surfaces of fcc crystals can be decomposed in microfacets with low Miller index (1 1 1), (1 0 0) or (1 1 0), corresponding to the terrace, step or kink according to their relative size. Decomposition for the Au(3 2 1) surface leads to: $Au(3\,2\,1) - [1_2(1\,1\,1) + 1_1(1\,1\,0) + 1_1(1\,0\,0)]$. This surface is composed of (1 1 1) terraces containing 2 unit cells, and steps and kinks of equal size with one unit cell each.

According to the same notation, Au(2 1 1) is decomposed in: Au(2 1 1) − [1$_2$(1 1 1) + 1$_1$(1 0 0)]. This surface has terraces and steps of equal size than Au(3 2 1) but no kinks.

The "fingerprints" of the Au{3 2 1}^{R} and Au{3 2 1}^{S} gold surfaces are presented in Fig. 1 and were obtained in 0.01 M $HClO_4$ following procedures described elsewhere [25]. The voltammetric profile is the same for both surfaces as expected. The pzc were obtained from the differential capacitance measurements. The difference between the values obtained for Au{3 2 1}^{R} (−120 mV) and Au{3 2 1}^{S} (−130 mV) are within experimental error. Such negative potential values are expected considering the roughness of the surface (a pzc value of −160 mV was obtained for the rough surface Au(2 1 0) in the same experimental conditions).

It is well established that gold single crystal surfaces are reconstructed under thermal or electrochemical treatment [27,31]. As reconstructed electrodes have a surface structure that may deviate considerably from that of the unreconstructed ones, we looked for the occurrence of thermally or electrochemically induced surface reconstruction, relaxation or faceting of the chiral surfaces following the usual procedures used for basal planes [32] and stepped surfaces [28] of gold. The voltammograms obtained in the double layer region for the chiral surfaces were stable from the first voltammetric scan and no effect of the negative and positive potential limit was observed, therefore indicating that reconstruction or faceting, if existent, is not significant under the experimental conditions used in this study. The lack of surface perturbation upon thermal or electrochemical treatment may arise from the fact that the dimensions of the flat domains existing on the Au(3 2 1) surfaces are too small to allow the surface reconstruction [31].

The results obtained for the electro-oxidation of glucose enantiomers were therefore analysed under the reasonable assumption that the gold chiral surface structure is identical to the ideal one. The same assumption was taken for electro-oxidation of glucose on the platinum chiral surfaces Pt{6 4 3} and Pt{5 3 1} based on electrochemical, LEED and AES experiments that showed that the high crystalline order of the surfaces was preserved [7]. Moreover, theoretical studies that predicted the roughening and relaxation of kinked platinum chiral surfaces with large flat domains [18,19], also pointed out that the structural disorder would not remove the net chirality of the surface. The same conclusion may be assumed in the case of gold substrates.

3.2. Structure sensitive oxidation of glucose on gold surfaces

The behaviour of the gold surface electrodes in solutions containing D- and L-glucose was studied using cyclic voltammetry in two different potential windows, [−0.7; 0.6 V] (short cycle) and [−0.7; 1.1 V] (full cycle that includes the surface oxidation). Consecutive potential scans were performed but no significant changes in the voltammetric curves were observed and the voltammetric profile was stable after the second cycle. The fifth cyclic voltammograms are presented in Fig. 2 for Au(1 1 1) in the L-glucose solution and supporting electrolyte alone. The profiles obtained show that

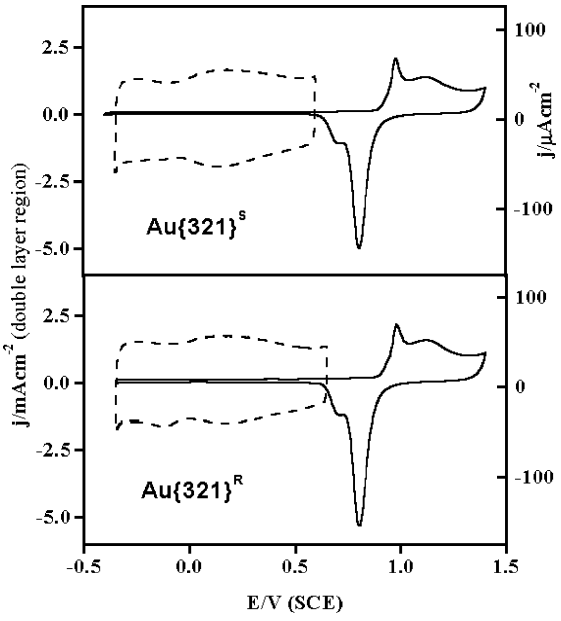

Fig. 1. "Fingerprints" of Au{3 2 1}^{R} and Au{3 2 1}^{S} surfaces obtained in 0.01 M $HClO_4$.

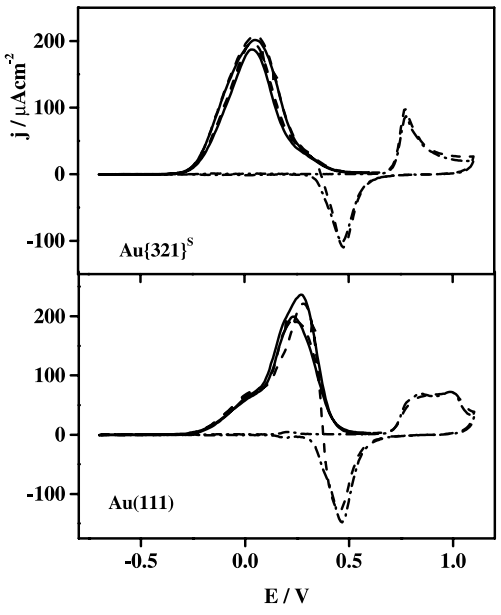

Fig. 2. Cyclic voltammograms obtained for Au(1 1 1) and Au{3 2 1}^{S} in supporting electrolyte alone (–·–·–) and 10 mM L-glucose with (- - - - - -) and without (——) extending the more positive potential to the surface oxidation region.

glucose is oxidized in the potential range [−0.3, 0.5 V] and that the oxidation is suppressed at higher potential values prior to the oxidation of the gold surface, likely due to competitive anion/water adsorption at high potentials. Comparison with the voltammogram obtained in the supporting electrolyte alone shows that the surface oxidation process is not affected by the previous oxidation of glucose meaning that neither glucose or its oxidation products are retained on the surface of the electrode. Once the gold oxide is reduced, the surface is reactivated for glucose oxidation to take place again. The profiles for the glucose oxidation in both direct and reverse scans are practically superimposed.

The absence of surface poisoning is confirmed by the analysis of the cyclic voltammograms obtained in the narrower potential window, if the potential is reversed before the surface oxidation takes place, the glucose oxidation is not inhibited and the profiles are also superimposed. These conclusions are valid for the other surfaces as well as for L-glucose oxidation. The absence of poisoning is a significant difference to that observed on platinum electrodes [33] in which extensive CO formation has been reported [34]. A slight increase of the glucose oxidation current is observed however for Au(1 1 1) which may be associated with the absence of defects that are usually formed during the surface oxidation [35]. Although the presence of such defects sometimes has major consequences on interfacial processes like for example 2D transition of adsorbed layers [36], it does not affect the glucose oxidation to a great extent. Fig. 2 shows that that surface oxidation of the already rough chiral surface Au{3 2 1}^{R} had no effect on the glucose oxidation.

3.3. Surface structure influence

Fig. 3 shows the cyclic voltammograms obtained for the four electrodes under study in D- and L-glucose solutions. A strong structural sensitivity is observed although common features are discernible suggesting that the overall glucose oxidation process must be similar irrespective of the surface structure. A Gaussian deconvolution of the profiles was performed assuming two major peaks for the glucose oxidation. Results of the deconvolution performed for D- and L-glucose oxidation in both positive and negative going sweeps are summarized in Table 1 and presented in Fig. 4 for the case of L-glucose in the positive going sweep.

The results show that the potential and current density of the two oxidation peaks depends on the surface crystallographic structure, and so does the onset of the glucose oxidation. The first faradaic peak corresponds to a reaction or path that is favoured by the presence of surface defects (steps or kinks), therefore its current density increases as the density of surface defects increases and its potential value is slightly more positive

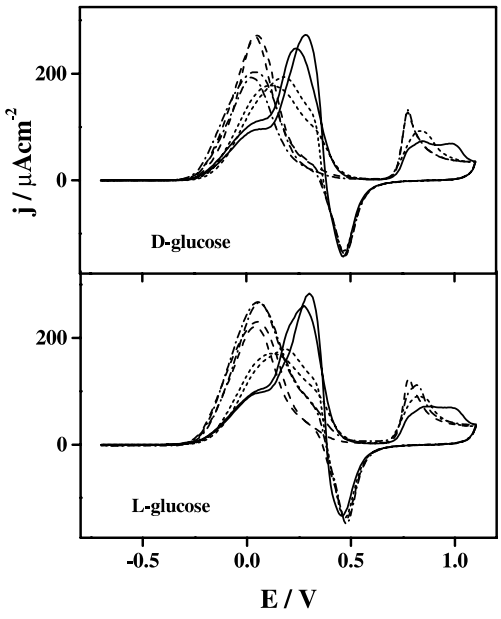

Fig. 3. Cyclic voltammograms obtained in 10 mM D- and L-glucose for the four faces under study: (——) Au (111), (- - - - - -) Au (211), (– – – –) Au{3 2 1}^{R} and (–·–·–·–) Au{3 2 1}^{S}.

for the smoother surfaces. The second reaction/path occurs more favourably on the ordered bidimensional domains (terraces) and therefore its current density increases as the density of surface defects decreases and its potential is more positive for the rougher surfaces. The onset of glucose oxidation is shifted to more negative values for the kinked surfaces.

3.4. Enantiomeric discrimination

To evaluate the enantiomeric effect, we compared the results obtained for D- and L-glucose oxidation for the four surfaces under study. This study is illustrated in Fig. 5 for one chiral surface, Au{3 2 1}^{R} and one non-chiral surface, Au(2 1 1). Although the voltammetric profiles obtained for each surface orientation are similar in shape for both isomers, same number of peaks at the same potential values, the current density of these peaks is affected by the intrinsic chirality of the surface.

For the non-chiral surfaces, Au(2 1 1) and also Au(1 1 1), the cyclic voltammograms are superimposed for both isomers, thus no enantiomeric effect is observed as expected. For Au{3 2 1}^{R}, the current observed for the oxidation of L-glucose is higher while the opposite situation is observed for Au{3 2 1}^{S} for which the oxidation of D-glucose leads to higher oxidation currents. The analysis of the two current peaks in Table 1 shows that both processes are affected by the chiral nature of the electrodes.

The chiral effect is also observed on the onset of glucose oxidation. Oxidation of D-glucose starts at

Table 1
Data from the voltammetric profiles obtained in the positive and negative going sweeps for the four gold surfaces under study in D- and L-glucose solutions

	Positive going sweep					Negative going sweep			
	E_{onset} (V/SCE)	E_{peak1} (V/SCE)	J_{peak1} ($\mu A\,cm^{-2}$)	E_{peak2} (V/SCE)	J_{peak2} ($\mu A\,cm^{-2}$)	E_{peak1} (V/SCE)	J_{peak1} ($\mu A\,cm^{-2}$)	E_{peak2} (V/SCE)	J_{peak2} ($\mu A\,cm^{-2}$)
D-Glucose									
Au(1 1 1)	−0.238	19	97	253	236	79	94	280	238
Au(2 1 1)	−0.199	101	177	315	54	91	145	250	101
Au(3 2 1)^{R}	−0.263	26	206	366	6	20	182	270	6
Au(3 2 1)^{S}	−0.246	40	264	334	18	39	251	259	25
Enantiomeric excess S %			−12		−50		−14		−60
L-Glucose									
Au(1 1 1)	−0.230	31	95	272	240	114	99	292	220
Au(2 1 1)	−0.192	103	170	322	57	132	168	287	46
Au(3 2 1)^{R}	−0.240	49	250	313	42	58	246	292	39
Au(3 2 1)^{S}	−0.259	39	214	345	13	53	202	282	17
Enantiomeric excess S %			8		53		10		39

The potential for the onset of the glucose oxidation was taken at $j > 10\ \mu A\,cm^{-2}$. Current densities for the oxidation peaks of glucose were obtained by Gaussian deconvolution.

lower potential values on Au{3 2 1}^{R} while oxidation of L-glucose starts at lower potential values on Au{3 2 1}^{S}.

The enantiomeric excess S is a measure of the enantioselectivity that can be calculated by the ratio of the difference in electro-oxidation currents (which is related to the reaction rates) over their sum for a given R and S surface at a fixed potential (E) [7]:

$$S = \frac{I_R - I_S}{I_R + I_S} \times 100\%. \quad (1)$$

The enantiomeric excess was evaluated in both the positive and negative going sweeps for D- and L-glucose using the current values obtained from the Gaussian deconvolution (see Table 1). The enantioselectivity obtained was quite low for the first peak, around 10%, and 50% for the second peak, although the current values for this peak are rather small and therefore more strongly affected by the experimental error.

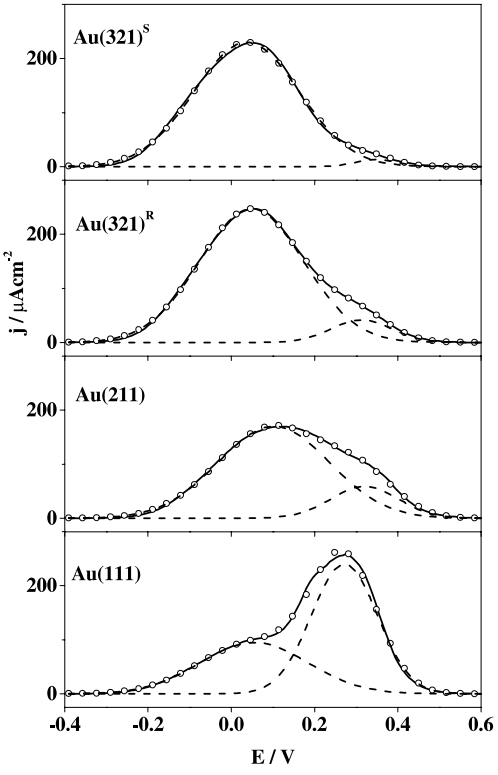

Fig. 4. Gaussian deconvolution of the cyclic voltammograms obtained for the four electrodes in L-glucose in the positive going sweep: (——) cyclic voltammogram, (- - - - - - -) adjusted curve, (○) result of the deconvolution.

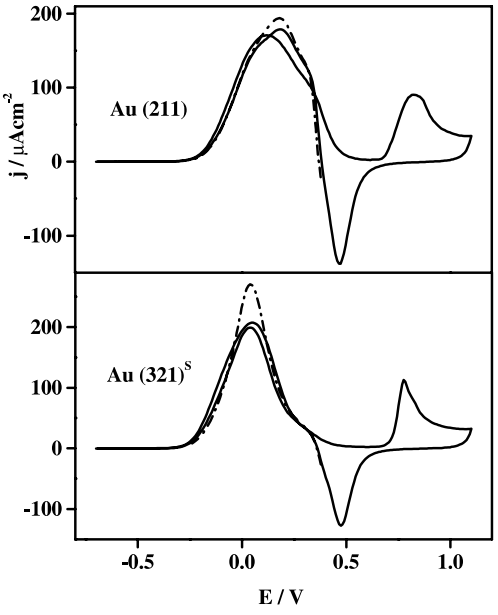

Fig. 5. Voltammograms obtained for Au(2 1 1) and Au{3 2 1}^{R} in (–·–·–) D- and (——) L-glucose.

4. Discussion and conclusions

According to the literature [22], the first step of the glucose oxidation in neutral or alkaline media involves the adsorption of glucose on the AuOH layer followed by the oxidation of the weakly bound hydrogen atom at the carbon C1 or the hydrogen of the hydroxyl group. The adradical that is formed reacts with AuOH formed in a fast reaction and glucolactone is formed and desorbed from the electrode. It is then hydrolysed in solution to form sodium gluconate.

The formation of $Au(OH)_{ads}$ on Au is the first step for the electrochemical oxidation of glucose. The chirality of the surfaces must be preserved since OH is a small molecule compared to the size of the kink site. The chiral site may then play a role in initially orienting the reactant molecules, and favour the adsorption of the radical according to its handedness in relation to the handedness of the kink. The actual bond-breaking and surface reaction, however, appear to proceed most likely by the same mechanism for all the surfaces.

It is noteworthy that the same type of reactivity was observed on chiral platinum surfaces: the R electrodes were more active towards D-glucose whereas the S electrodes were more reactive towards L-glucose [5] and vice versa. This result could not be predicted a priori and suggests similar adsorption steps in bot metal surfaces, despite their well-known differences as electrocatalizers.

We are presently performing studies on the oxidation of glucose isomers in alkaline media. It is indeed well known that increasing the medium pH enhances the glucose oxidation, therefore we expect that the enantiomeric effect will be amplified and will led to higher a enantiomeric excess. It is also expected that the chiral effect will scale with the increasing density of chiral defects as already reported in the literature for the oxidation of glucose isomers on platinum chiral surfaces [5]. A thorough study using other gold surfaces with variable density and orientation of surface chiral sites is necessary to better evaluate the role played by the chiral kink sites on the overall electro-oxidation of the glucose isomers.

Acknowledgements

A.M. and A.Q. would like to thank the FCT for financial support and grant (Project POCTI QUI/41704/2001). A.M. is grateful to A. Hamelin (CNRS-Meudon) for the preparation of the non-chiral gold single crystals. This work was carried out at CIQ-UP, Linha 4.

References

[1] M. Jacoby, C&EN March 25 (2002) 43.
[2] Y. Orito, S. Imai, S. Nina, J. Chem. Soc. Japan 8 (1979) 1118.
[3] G.A. Attard, J. Clavilier, J.M. Feliu, in: J.M. Hicks (Ed.), Chirality: Physical Chemistry, ACS Symposium Series No. 810, 2002 (Chapter 18).
[4] C.F. McFadden, P.S. Cremer, A.J. Gellman, Langmuir 12 (1996) 2483.
[5] A. Ahmadi, G. Attard, J. Feliu, A. Rodes, Langmuir 15 (1999) 2420.
[6] G. Attard, A. Ahmadi, J. Feliu, A. Rodes, E. Herrero, S. Blais, G. Jerkiewicz, Phys. Chem. B 103 (1999) 1381.
[7] G.A. Attard, J. Phys. Chem. B 105 (2001) 3158.
[8] G.A. Attard, C. Harris, E. Herrero, J. Feliu, Faraday Discuss. 121 (2002) 253.
[9] G.A. Attard, J.E. Gillies, C.A. Harris, D.J. Jenkins, P. Johnston, M.A. Price, D.J. Watson, P.B. Wells, Appl. Catal. A 222 (2001) 393.
[10] D.J. Watson, G.A. Attard, Electrochim. Acta 46 (2001) 3157.
[11] J.D. Horvath, A.J. Gellman, J. Am. Chem. Soc. 123 (2001) 7953.
[12] A.J. Gellman, J.D. Horvath, M.T. Buelow, J. Mol. Catal. A 167 (2001) 3.
[13] J.D. Horvath, A.J. Gellman, J. Am. Chem. Soc. 124 (2002) 2384.
[14] D.S. Sholl, Langmuir 14 (1998) 862.
[15] T.D. Power, D.S. Sholl, Vac. Sci. Technol. A 17 (1999) 1700.
[16] D.S. Sholl, A. Asthagiri, T.D. Power, J. Phys. Chem. B 105 (2001) 4771.
[17] A. Asthagiri, P.F. Feibelman, D.S. Sholl, Top. Catal. 18 (2002) 193.
[18] T.D. Power, D.S. Sholl, Top. Catal. 18 (2002) 201.
[19] T.D. Power, A. Asthagiri, D.S. Sholl, Langmuir 18 (2002) 3737.
[20] B. Beden, I. Çetin, A. Kahyaoglu, D. Takky, C. Lamy, J. Catal. 104 (1987) 37.
[21] R.R. Adžić, M.W. Hsiao, E.B. Yeager, J. Electroanal. Chem. 260 (1989) 475.
[22] M.W. Hsiao, R.R. Adžić, E.B. Yeager, J. Electrochem. Soc. 143 (1996) 759.
[23] Ž. Žljivančanin, K.V. Gothelf, B. Hammer, J. Am. Chem. Soc. 149 (2002) 14789.
[24] J. Clavilier, D. Armand, S.G. Sun, M. Petit, J. Electroanal. Chem. 205 (1986) 267.
[25] A. Hamelin, in: B.E. Conway, R.E. White, J.O'M. Bockris (Eds.), Modern Aspects of Electrochemistry, vol. 16, Plenum Press, New York, 1985 (Chapter 1).
[26] A. Hamelin, S. Morin, J. Richer, J. Lipkowski, J. Electroanal. Chem. 285 (1990) 249, appendix.
[27] A.S. Dakkouri, D.M. Kolb, in: A. Wieckowski (Ed.), Interfacial Electrochemistry: Theory, Experiment, and Applications, Marcel Dekker, New York, 1999 (Chapter 10).
[28] A.F. Silva, A. Martins, J. Electrochim. Acta 44 (1998) 919.
[29] R.T. Morrison, R.N. Boyd, Organic Chemistry, third ed., Allyn and Bacon, Boston, 1973.
[30] M.A. Van Hove, G.A. Somorjai, Surf. Sci. 92 (1980) 489.
[31] A.F. Silva, A. Martins, in: A. Wieckowski (Ed.), Interfacial Electrochemistry: Theory, Experiment, and Applications, Marcel Dekker, New York, 1999 (Chapter 25).
[32] A. Hamelin, J. Electroanal. Chem. 407 (1996) 001.
[33] M.J. Llorca, J.M. Feliu, A. Aldaz, J. Clavilier, A. Rodes, J. Electroanal. Chem. 316 (1991) 175.
[34] A. Rodes, M.J. Llorca, J.M. Feliu, J. Clavilier, An. Quim. Int. Ed. 92 (1996) 118.
[35] H. Honbo, S. Sugawara, K. Itaya, Anal. Chem. 62 (1990) 2424.
[36] A.F. Silva, M.J. Sottomayor, A. Martins, J. Electroanal. Chem. 375 (1994) 395.